

## Preparation and properties of polymerizable 1,8-naphthalimide fluorescent dye grafted linear low-density polyethylene

Zesen Lin,<sup>1,2</sup> Jianfu Zhang,<sup>3</sup> Haifeng Ma,<sup>3</sup> Zhanhai Yao<sup>1</sup>

<sup>1</sup>State Key Laboratory of Polymer Physics and Chemistry, Changchun Institute of Applied Chemistry, Chinese Academy of Sciences, Changchun 130022, People's Republic of China

<sup>2</sup>University of Chinese Academy of Sciences, Beijing 100049, People's Republic of China

<sup>3</sup>College of Chemistry and Environmental Engineering, Changchun University of Science and Technology, Changchun, People's Republic of China

Correspondence to: Z. H. Yao (E-mail: yaozh@ciac.ac.cn)

**ABSTRACT:** Light converting greenhouse films are novel plastic films for agriculture. In this study, 4-methoxy-N-allyl-1,8-naphthalimide (MOANI) was grafted onto linear low-density polyethylenes (LLDPE-g-MOANI) by melt reactive mixing. The effects of monomer concentration, chamber temperature, and reaction time on grafting degree were systematically studied. Evidence of the grafting reaction was determined by <sup>1</sup>HNMR, FTIR, UV-Vis, and fluorescence spectrometry. Dynamic rheological properties, isothermal crystallization kinetics, surface morphologies of LLDPE, LLDPE-g-MOANI, and blends of LLDPE and MOANI (LLDPE/MOANI) were also analyzed. In addition, mechanical and fluorescent properties of unpurified LLDPE-g-MOANI films were further studied after the UV condensation weathering and acceleration migration test, respectively. We demonstrated that the cross-linking of LLDPE could be inhibited effectively by the graft of MOANI; the grafted MOANI acted as a nucleation agent to accelerate crystallization; the grafted MOANI effectively inhibited the aging process of LLDPE and the migration of free MOANI to the surface of the unpurified LLDPE-g-MOANI film. The modified LLDPE showed the potential application in long-term light converting films. © 2015 Wiley Periodicals, Inc. *J. Appl. Polym. Sci.* **2015**, *132*, 42172.

**KEYWORDS:** dyes/pigments; grafting; irradiation; polyolefins; synthesis and processing

Received 5 December 2014; accepted 4 March 2015

DOI: 10.1002/app.42172

### INTRODUCTION

The global solar radiation which reaches the Earth's surface contains ultraviolet (UV), photosynthetically active radiation (PAR, 400–700 nm), and near-infrared (NIR). However, plant growth and photosynthesis depend mainly on PAR and most plants have maximum photosynthetic sensitivity in the blue-violet and red-orange regions (400–500 and 600–700 nm).<sup>1,2</sup> In addition, UV can impair photosynthesis in many plants and especially UV-A (320–400 nm) can significantly decrease photosynthetic parameters by more than 70%.<sup>3</sup> Light converting greenhouse films are agricultural plastic films for shifting inactive solar radiation to light for photosynthesis by adding fluorescent colorants into the film,<sup>4,5</sup> and undoubtedly, the material used for these films widely is polyethylene.<sup>6</sup> Thus, these films can enhance crop productivity, advance harvest time, and save energy.<sup>2,7–9</sup>

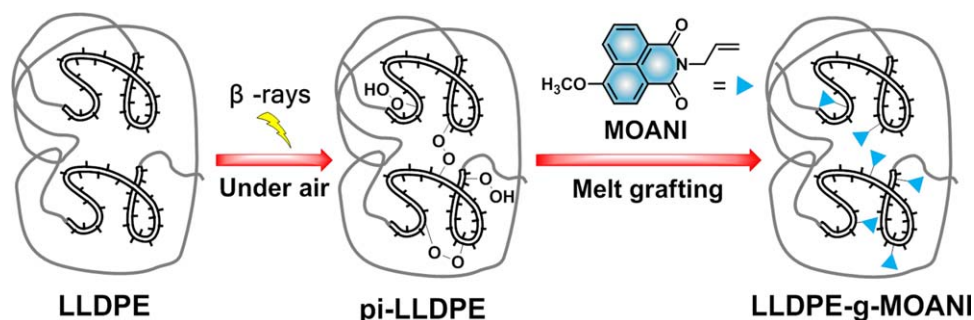
Fluorescent colorants for light converting greenhouse films include the following: inorganic pigments of rare earth elements, rare earth

complex dyes with organic ligands, and fluorescent organic dyes. Inorganic pigments of rare earth elements are dispersed hard uniformly into polyethylene unless its surface is modified;<sup>10</sup> the light and heat stability of rare earth complex dyes are inadequate;<sup>11</sup> fluorescent organic dyes are molecular dispersion in the polymer, more thermostable than rare earth complex dyes, safer about environment,<sup>12</sup> and cheaper than rare earth type fluorescent colorants.

Unfortunately, fluorescent organic dyes lack an affinity for aliphatic hydrocarbons, consequently migrate to the surface of polyolefins,<sup>10,13</sup> and even crystallize on the surface (namely blooming effect<sup>14</sup>). Many attempts have been made over decades to improve the dyeability of polyolefins and avoid dye migration in polyolefins including the following: (1) blending of polyolefins with polar polymers, dendrimers, and hyperbranched polymers;<sup>13</sup> (2) the encapsulation of the dye in core-shell nano- or microparticles;<sup>14</sup> (3) polymeric dye, obtained by copolymerization of a functionalized dye with given monomers, such as acrylic monomers.<sup>15–18</sup>

Additional Supporting Information may be found in the online version of this article.

© 2015 Wiley Periodicals, Inc.



**Scheme 1.** Pre-irradiation-induced graft polymerization of MOANI onto LLDPE. [Color figure can be viewed in the online issue, which is available at [wileyonlinelibrary.com](http://wileyonlinelibrary.com).]

However, many issues such as the steps of complex, high cost, and difficult continuous production exist in the above methods. The preirradiation and reactive extrusion grafting joint technology is an effective, low-cost, suitable for industrial production polyethylene modification method.<sup>19</sup> This technology can avoid the cross-linking of polyethylene compared with the traditional irradiation method.<sup>19</sup> During the last years, many efforts have been made to modify polyethylene with this method,<sup>19–21</sup> whereas no attempt has been made as yet to graft polymerizable dye onto polyethylene.

4-Alkoxy and 4-acylamino derivatives of 1,8-naphthalimide are well used as fluorescent brightening agents for polymers with an intensive blue fluorescence, such as Mikawhite AT.<sup>22</sup> Therefore, these derivatives are also suitable for a fluorescent colorant for light converting greenhouse films.

In this study, we synthesized 4-methoxy-N-allyl-1,8-naphthalimide<sup>23</sup> (denoted as MOANI) using a one-pot method (Scheme S1) and grafted it onto preirradiated linear low-density polyethylene (LLDPE) with a melt reactive mixing process (Scheme 1), and characterized spectral, thermo, and rheological properties of the grafted copolymer (denoted as LLDPE-g-MOANI) obtained in mixer after purification. In order to demonstrate no blooming effect for the LLDPE-g-MOANI, surface morphologies of LLDPE-g-MOANI and the blends of MOANI and LLDPE (denoted as LLDPE/MOANI) were examined by scanning electron microscope (SEM). In addition, accelerated migration and UV weathering of blown films of unpurified LLDPE-g-MOANI obtained in extruder were tested since in actual industrial production, the purification process will not be used. These tests can demonstrate that migration of the free MOANI in unpurified LLDPE-g-MOANI films was delayed by the grafted MOANI in these films.

## EXPERIMENTAL

### Materials

The LLDPE powder (DFDA-7042) was supplied by Jilin Petrochemical Co., People's Republic of China, and was used without additives with a melt flow rate (MFR) 2.0 g/10 min and a density of 0.918 g cm<sup>-3</sup>. 4-Chloro-1,8-naphthalic anhydride (CNA, 94% purity/GC), allylamine hydrochloride (>98%), sodium methylate (30 wt % methanol solution, ca 5 mol L<sup>-1</sup>), and deuteration chloroform-D<sub>1</sub> [99.8% atom % D contains 0.1% (v/v) TMS] were purchased from alfa aesar, TCI, Aladdin, and

Beijing Chongxi Fine Chemical High-Tech Business Incubator Co., Ltd, respectively. Other reagents and solvents were of analytical grade and were purchased from Beijing Chemicals Co., China. All reagents and solvents were used without further purification.

### Instruments

The melting point and other thermal properties were measured from a differential scanning calorimetry (Perkin-Elmer DSC-7). Mass spectra and purity were determined with an Agilent 5975 gas chromatograph/mass spectrometer (GC/MS) systems. <sup>1</sup>H NMR and <sup>13</sup>C NMR were recorded on a Bruker AV 400 or 600 NMR spectrometer. Infrared spectrum was recorded with a Bruker Vertex 70 Fourier transform infrared spectrometer, and each spectrum was recorded from 400–4000 cm<sup>-1</sup> with a total of 32 scans. A Perkin-Elmer Lambda 900 UV/Vis/NIR spectrometer and HITACHI F-7000 fluorospectrometer was employed for the absorbance and fluorescence studies, respectively. The rheological properties were measured using a TA ARES-G2 rheometer on which a 25-mm-diameter aluminum parallel plate was mounted.

The preparation of LLDPE-g-MOANI and LLDPE/MOANI took place in a HAPRO Mix-60C mixer with an effective volume of 60 mL and two Roller rotors. The speed ratio of two rotors is 3 : 2.

The master batch of LLDPE-g-MOANI or LLDPE/MOANI was prepared using a HAPRO EP-20–25C single-screw extruder connected to a rod capillary die. The diameter of the screws was 20 mm and the ratio of length to diameter (L/D) was 25. The barrel of the extruder is divided into three zones and each zone of the barrel and die is heated independently.

Blown films were prepared using a HAPRO EP-20–25C single-screw extruder connected to a blown film die and HAPRO FB-300 plastic film blowing machine. The blown film was then cooled by wind ring. The die diameter is 24 mm and the ring gap of die is 0.3–1.8 mm.

The study on the UV weathering of films was performed in an Atlas UV Test fluorescent UV condensation weathering device with fluorescent UV lamps (UVA 340 nm, 40 W).

### One-Pot Synthesis of 4-Methoxy-N-Allyl-1,8-Naphthalimide (MOANI)

A mixture of 4-chloro-1,8-naphthalic anhydride (25.0000 g, 107 mmol), allylamine hydrochloride (12.0650 g, 129 mmol), and triethylamine (TEA, 22.5 mL, 161 mmol) were refluxed in 470 mL of methanol for 2 h. The solution was cooled to 45°C and then

sodium methylate solution ( $\text{CH}_3\text{ONa}/\text{CH}_3\text{OH}$ , 195.5 mL, 978 mmol), copper sulfate pentahydrate (3.2200 g, 12.9 mmol), and methanol of 30 mL were added. The mixture was heated to reflux for 2 h. Subsequently, the above mixture poured in 1 L  $2 \text{ mol L}^{-1}$  muriatic acid and the precipitate collected by suction filtration. After washing of the residue with  $2 \text{ mol L}^{-1}$  muriatic acid and water, the solvent removed in vacuo at  $80^\circ\text{C}$  to give MOANI as yellow precipitate in 90% yield. Recrystallization from methanol gave yellow needles, mp  $118\text{--}122^\circ\text{C}$  (DSC, Supporting Information Figure S1, lit.  $119\text{--}120^\circ\text{C}^{24}$ ), purity 97.3% (GC);  $^1\text{H}$  NMR (400 MHz, Chloroform- $d$ ,  $\delta$ ) 8.64 (d,  $J = 7.2$  Hz, 1H, Ar H), 8.60 (d,  $J = 8.3$  Hz, 2H, Ar H), 7.73 (t,  $J = 7.8$  Hz, 1H, Ar H), 7.08 (d,  $J = 8.3$  Hz, 1H, Ar H), 6.08–5.96 (m, 1H; CH=), 5.33 (d,  $J = 17.0$  Hz, 1H;  $\text{CH}_2=$ ), 5.21 (d,  $J = 10.3$  Hz, 1H;  $\text{CH}_2=$ ), 4.82 (d,  $J = 5.7$  Hz, 2H;  $\text{CH}_2$ ), 4.15 (s, 2H;  $\text{CH}_3$ );  $^{13}\text{C}$  NMR (151 MHz, DMSO,  $\delta$ ): 163.36 (C=O), 162.71 (C=O), 160.51 (Ar C), 133.49 (Ar C), 133.01 (Ar C), 131.22 (CH=), 128.72 (Ar C), 128.46 (Ar C), 126.52 (Ar C), 122.91 (Ar C), 121.92 (Ar C), 116.28 ( $\text{CH}_2=$ ), 114.23 (Ar C), 106.42 (Ar C), 56.72 ( $\text{CH}_3$ ) 41.62 ( $\text{CH}_2$ ); IR(KBr): 3076 (w), 3013 (w), 2949 (w), 1690 (s; imide C=O), 1657 (s; imide C=O), 1593 (s; ring C=C), 1579 (s; ring C=C), 1514 (m), 1382 (s), 1348 (s), 1269 (s), 1239 (s), 1097 (s;  $\nu_{\text{as}}(\text{C—O—C})$ ), 1071 (m), 917 (m),  $780 \text{ cm}^{-1}$  (s;  $\omega(\text{Ar C—H})$ ); UV–Vis (ethanol):  $\lambda_{\text{max}}(\epsilon) = 365 \text{ nm}$  (12220); fluorescence (ethanol):  $\lambda_{\text{max}}^{\text{fl}} = 442 \text{ nm}$ ; EIMS ( $m/z$  (%)) 267 (34) [ $M^+$ ], 252 (100) [ $M - \text{CH}_3$ ] $^+$ .

#### Preparation of Preirradiated LLDPE

LLDPE was preirradiated by the electron beam (EB) in the air at room temperature using a DD-3.0 Dynamitron electron accelerator (Jiangsu Dasheng Electron Accelerator Co., Ltd.), with the electron energy of 3 MeV, dose rate of  $7 \text{ kGy s}^{-1}$  and total dose of 12 kGy, respectively. The beam length is 7.5 cm and the scanning width of beam is 1.2 cm. The beam current was kept constant to a value of 7.2 mA beam current and the conveyor speed was set to  $4.8 \text{ m min}^{-1}$ . Both hydroperoxide and peroxides (POOH and POOP) were generated on the LLDPE backbone.<sup>25,26</sup>

#### Preparation of LLDPE-g-MOANI for Study of Grafting Degree (GD)

The preparation of LLDPE-g-MOANI took place in a HAPRO Mix-60C mixer with an MOANI concentration of 0.5 wt % based on preirradiated LLDPE as 100 wt % at  $190^\circ\text{C}$  and 60 rpm for 7 min. By adjusting monomer concentration (0.5–3 wt %), processing temperature (from 150 to  $225^\circ\text{C}$ ), and reaction time (from 1.5 to 9.5 min), LLDPE-g-MOANI were obtained with different degree of grafting.

#### Purification of Reaction Product

Purification of the graft copolymer is required before study of GD. The purpose of purification is to remove unreacted monomer and other byproducts of the reaction.

Five grams of grafted LLDPE was dissolved in 300 mL of toluene, and then the solution was poured into 400 mL of acetone under stirring. The precipitate was filtered, washed with acetone several times, and dried in vacuum oven at  $60^\circ\text{C}$  for 24 h to give the purified LLDPE-g-MOANI. From now on, we will define the designation LLDPE-g-MOANI as the purified material from that obtained from mixer, which is called “unpurified”.

#### Characterization of LLDPE-g-MOANI for Study of GD

The LLDPE-g-MOANI was analyzed by UV/Vis, FTIR spectrometer, and fluorospectrometer. The specimens were compression-molded into films of  $0.11 \pm 0.02 \text{ mm}$  in thickness at  $200^\circ\text{C}$ . The UV/Vis spectra from 250 to 600 nm were recorded with air as blank. The absorbance of every film in the maximum absorption wavelength was the average of three measurements at different zones. The fluorescence spectra from 380 to 600 nm were recorded using front-surface fluorometry at 358 nm as the excitation wavelength, 700 V photomultiplier tube (PMT) voltage, and  $1200 \text{ nm min}^{-1}$  scan speed. The FTIR spectra from 400 to  $4000 \text{ cm}^{-1}$  were recorded with a total of 32 scans and the resolution was  $4 \text{ cm}^{-1}$ . The evidence of grafting was determined by  $^1\text{H}$  NMR. The LLDPE-g-MOANI and LLDPE spectra were recorded on a Bruker AV 400 NMR spectrometer at  $110^\circ\text{C}$  in  $o$ -dichlorobenzene- $d_4$ .

Dynamic rheological properties of melts of LLDPE-g-MOANI, LLDPE, and preirradiated LLDPE were measured in small amplitude oscillatory shear (SAOS) tests using a TA ARES-G2 rheometer on which a 25-mm-diameter aluminum parallel plate was mounted. Samples of the LLDPE and LLDPE-g-MOANI were molded into discs of 25 mm diameter and 1 mm thickness at  $200^\circ\text{C}$ . The storage modulus [ $G'(\omega)$ ] and the loss modulus [ $G''(\omega)$ ] were determined at  $190^\circ\text{C}$  and at frequencies ( $\omega$ ) ranging from 0.1 to  $500 \text{ rad s}^{-1}$ . The curves of  $G'(\omega)$  and  $G''(\omega)$  versus  $\omega$  were the average of three measurements. The strain amplitude was set at 5% and checked to be within linear viscoelastic range by strain sweeps. The tests were performed under nitrogen atmosphere to avoid degradation of samples.

Thermal properties of LLDPE-g-MOANI were measured from a DSC. Each sample was melted in the calorimeter at  $170^\circ\text{C}$ , hold for 1 min to erase the thermal history, then cooled to  $20^\circ\text{C}$ , and reheated to  $170^\circ\text{C}$ . The scan rate was  $10^\circ\text{C min}^{-1}$  on heating and cooling. The crystallization peak, melting peak, and the area of the endotherm were determined to give the crystallization temperature ( $T_c$ ), the melting temperature ( $T_m$ ), and enthalpy ( $\Delta H_c$ ,  $\Delta H_m$ ).

The surface morphologies of the LLDPE-g-MOANI and LLDPE/MOANI films were characterized by a FEI XL30 field emission scanning electron microscope (FESEM). Micrographs were taken at a 10-kV acceleration voltage. The specimens were compression-molded into films of  $0.11 \pm 0.02 \text{ mm}$  in thickness at  $200^\circ\text{C}$  and were stored for 3 months at room temperature after the cooling stage. Before SEM observations, the surfaces of specimens were coated with a thin layer of gold to avoid electrical charging and increase contrast during observation.

#### Preparation of Unpurified LLDPE-g-MOANI and LLDPE/MOANI Films

The master batch of unpurified LLDPE-g-MOANI of LLDPE/MOANI of 1 wt % was prepared and then blended with LLDPE to materials of different concentrations, with the formulation and process conditions summarized in Table I using above-mentioned single-screw extruder.

Blown film (thickness was  $0.10 \pm 0.02 \text{ mm}$ ) was prepared from the unpurified LLDPE-g-MOANI or LLDPE/MOANI of different concentrations. The rotor speed was 60 rpm and the

**Table I.** Formulation and Process Conditions of the Reactive Extrusion

Experiment number	PE type	Composition (wt %)			Temperature (°C)				Rotor speed (rpm)
		MOANI	PE	1% master batch	$T_1$	$T_2$	$T_3$	$T_d$	
1	pi-LLDPE	1	99	-	150	190	200	210	20
2	LLDPE	-	95	5					50
3	LLDPE	-	85	15					50
4	LLDPE	-	75	25					50
5	LLDPE	1	99	-					20
6	LLDPE	-	85	15					50

temperature was 150, 190, 200, and 210°C from feed throat to die, respectively. The blow-up ratio (BUR) and drawn-down ratio (DDR) were 2.6 and 1.1, respectively. Corresponding calculation formulas of BUR and DDR was referenced from the book written by Harper.<sup>27</sup>

#### Test of Accelerated Migration of MOANI in Films

The most important influence factor to migration of polar additives in PE greenhouse films is water vapor from the transpiration of plants, so we simulated greenhouse using an 8302 Acceleration Dripping Tester (Gongyi Yuhua Co., Ltd., China) at 60°C. The acceleration dripping tester is a water bath with a cover which has six round holes in 13 cm diameter for covering films for measurement of dipping properties of PE greenhouse films.<sup>19</sup> Every once in a while, fluorescence spectra of films were recorded [excitation wavelength ( $\lambda_{ex}$ ): 358 nm, PMT voltage: 500 V, scan speed: 1200 nm min<sup>-1</sup>] and the fluorescence intensity of every film in the maximum emission wavelength was the average of three to five for at least 3 measurements at different zones.

#### Test of UV Weathering of Films

The study on the UV weathering of films was performed and a test cycle included 8 h UV at 60 ( $\pm 3$ )°C black panel temperature with 0.8 W m<sup>-2</sup> irradiance, 3.75 h condensation at 45 ( $\pm 3$ )°C black panel temperature, 0.25 h spray, and 12h dark. Films were tailored to the rectangle with 12 cm length and 7.5 cm width as specimens.

Every 1–3 days, a group of specimens of films were taken out from the weathering device, fluorescence spectra of the group of specimens were recorded (EX WL: 358 nm, PMT voltage 450 V, scan speed: 1200 nm min<sup>-1</sup>), and the fluorescence intensity of every film in the maximum emission wavelength was the average of three measurements at different zones, and then tensile tests of films were carried out in an INSTRON 1211 tensile compression testing machine at room temperature and speed of 50 nm min<sup>-1</sup> with the specimen type 5 according to the ISO 527-3 standard.<sup>28</sup> The tensile strength and elongation at break of films were the average of three measurements.

## RESULTS AND DISCUSSION

### Spectra of LLDPE-g-MOANI and Proof of MOANI Grafted on LLDPE

The UV/Vis absorption and fluorescence emission spectra of the LLDPE-g-MOANI and MOANI are shown in Figure 1 (a,b).

That the absorption and emission of MOANI appear at the range of 300–600 nm indicates that MOANI has been successfully grafted onto the LLDPE backbone, because the purification of unpurified LLDPE-g-MOANI has been done before spectrum test and this procedure has been considered to be effective in past other related researches.<sup>29–31</sup> Besides, the FTIR spectra

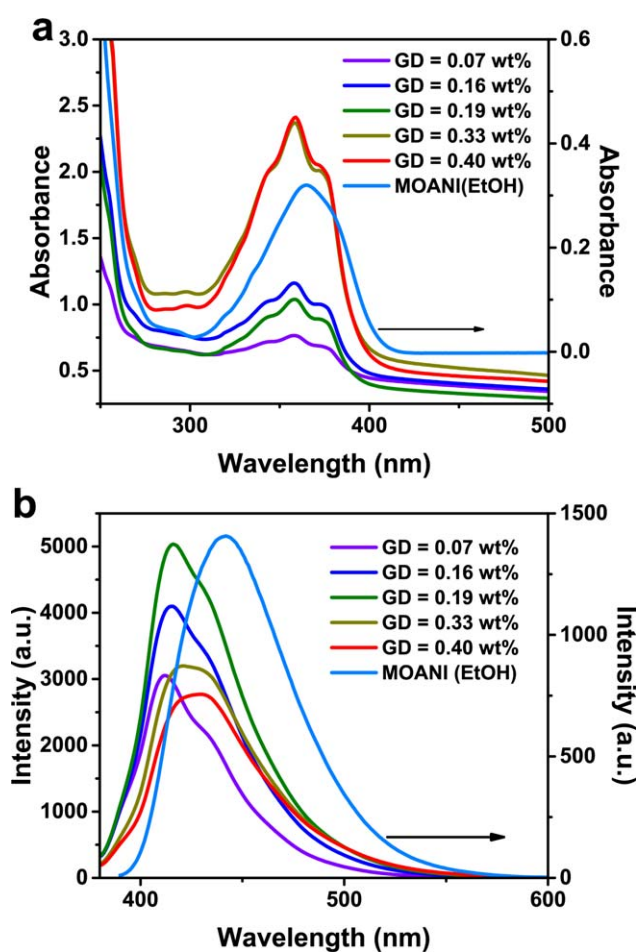


**Figure 1.** (a) Absorption spectra of MOANI in the EtOH ( $2.619 \times 10^{-5}$  mol L<sup>-1</sup>) and LLDPE-g-MOANI at room temperature; (b) Fluorescence spectra of MOANI in the EtOH ( $2.619 \times 10^{-5}$  mol L<sup>-1</sup>) and LLDPE-g-MOANI at  $\lambda_{ex} = 358$  nm and room temperature. [Color figure can be viewed in the online issue, which is available at wileyonlinelibrary.com.]

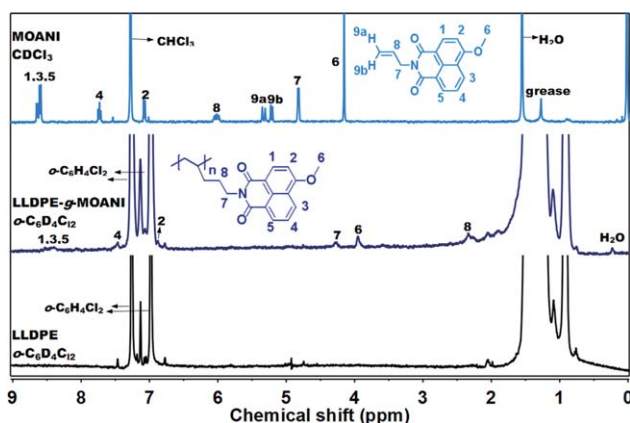


**Figure 2.**  $^1\text{H-NMR}$  spectra of the plain LLDPE, LLDPE-g-MOANI (GD=0.4 wt %), and MOANI. [Color figure can be viewed in the online issue, which is available at [wileyonlinelibrary.com](http://wileyonlinelibrary.com).]

[Supporting Information Figure S3] prove the occurrence of graft reaction between MOANI and preirradiated LLDPE again. Comparing the spectra of LLDPE-g-MOANI and MOANI, the Stokes shift of LLDPE-g-MOANI is smaller 30 nm than that of MOANI in alcohol, as a result of the solvatochromism.<sup>32,33</sup> Otherwise, absorption and emission of LLDPE-g-MOANI and LLDPE/MOANI show no significant difference [Supporting

Information Figure S2], which strongly suggest that the group at the nitrogen of imide almost has no effect on the spectral property of naphthalene.<sup>18</sup> The appearance of several absorption peaks or shoulders for chromophores in LLDPE-g-MOANI is attributed to that LLDPE is rigid medium relative to alcohol at room temperature.<sup>33</sup>

$^1\text{H-NMR}$  spectra of the LLDPE, LLDPE-g-MOANI, and MOANI are shown in Figure 2, respectively. Peaks of allyl does not appear at the range of 4–7 ppm in the spectrum of LLDPE-g-MOANI and several new peaks appear at the range of 1.5–3 ppm relative to LLDPE and MOANI. This result was further evidence that MOANI was grafted on LLDPE.

#### Determination of GD and GE of LLDPE-g-MOANI

GD was determined by UV/Vis spectra. The reason selecting this method and detailed procedures establishing the calibration equation was shown in Supporting Information. A linear calibration curve [Figure 3(a)] was established and the calibration equation could be obtained and shown as follows:

$$C_m = 0.1012 \times \frac{A_{358}}{A_{450}} - 0.1330 \quad (1)$$

where  $C_m$  denotes the monomer concentration,  $A_{358}$  and  $A_{450}$  are absorbance at maximum absorption wavelength of MOANI

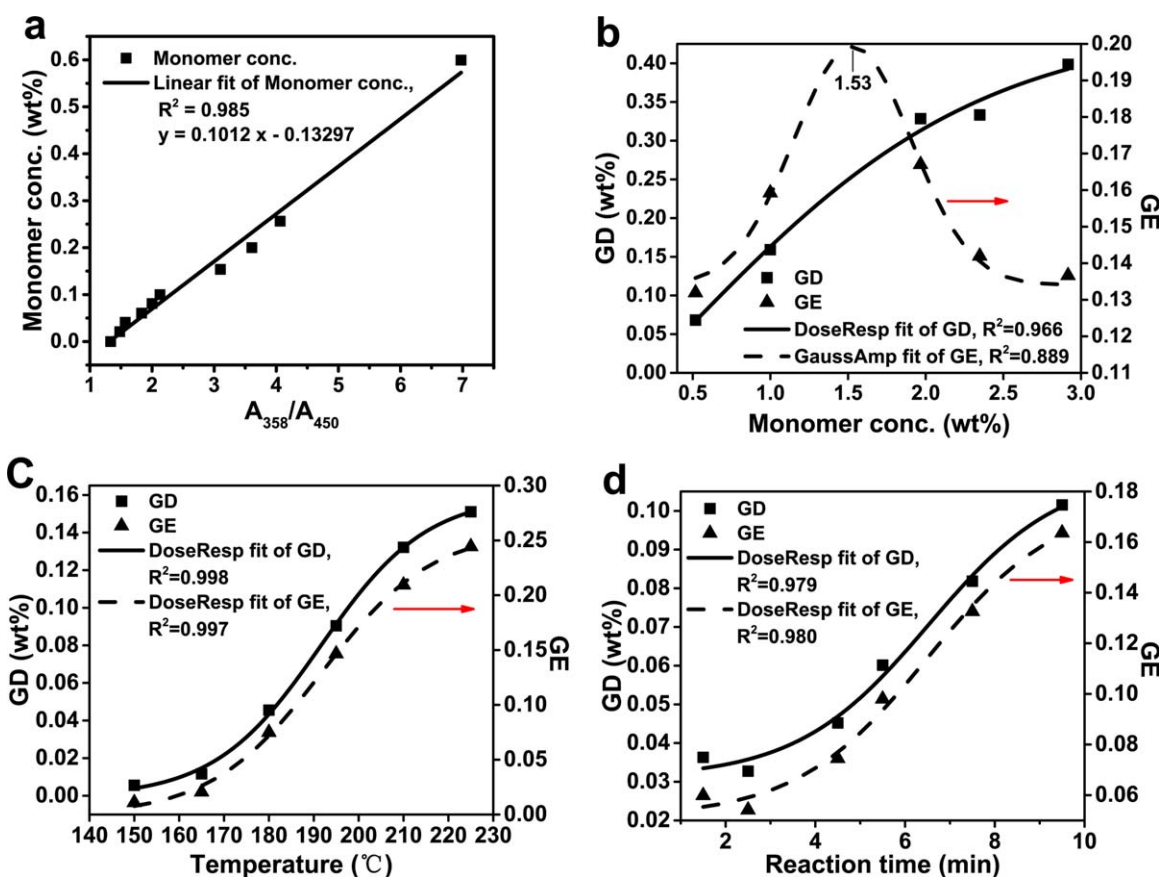


**Figure 3.** (a) The relationship between the absorbance ratio ( $A_{358}/A_{450}$ ) and monomer concentration (the calibration curve); (b–d) Effect of reaction time, temperature, and initial monomer concentration on grafting degree (GD) of LLDPE-g-MOAN, respectively. [Color figure can be viewed in the online issue, which is available at [wileyonlinelibrary.com](http://wileyonlinelibrary.com).]

and baseline absorbance of LLDPE, respectively. Intercept of the calibration equation is caused by the tilted baseline of the plain LLDPE [Supporting Information Figure S2(a)].

GD and grafting efficiency (GE) of the purified LLDPE-g-MOANI is determined by following equations:

$$GD = C_p \quad (2)$$

$$GE = \frac{M_p}{M_I} = \frac{GD}{C_I} \quad (3)$$

where  $C_p$ ,  $C_I$ ,  $M_p$ , and  $M_I$  denotes the concentration of grafted and initial monomers and the mass of grafted and initial monomers, respectively.

### Effect of Processing Parameters on GD and GE

**Effect of Initial Monomer Concentration.** Initial monomer concentration is one of the main process parameters for controlling the GD. With an increase in the monomer concentration, GD and GE would increase [Figure 3(b)], when initial monomer concentration was less than 1.5%. The generation rate of macroradicals unvarying at a certain temperature and content of macromolecule peroxides, the possibility and rate of grafting reaction is increasing with increasing initial monomer concentration. The LLDPE-g-MOANI did not contain the gel. This shows that the cross-linking could be avoided during the grafting reaction of monomer onto low-dose preirradiated LLDPE. When initial monomer concentration exceeds 1.5%, macroradical concentration reduced remarkably owing to macroradicals reacted with large amount of monomer rapidly. The rate of grafting reaction was decreasing with further increasing of monomer concentration, as a result of slow growth of GD gradually and decrease of GE.

**Effect of Chamber Temperature.** Chamber temperature is one of the other main process parameters for controlling the GD. It can be seen that GD and GE of LLDPE-g-MOANI increase with an increasing chamber temperature [Figure 3(c)]. According to Arrhenius equation, this result could be explained as increased thermal decomposition rate of peroxide on the preirradiated LLDPE backbone with increasing chamber temperature, leading to increased LLDPE macroradicals concentration, and thus enhanced the degree of grafting. Another factor can be faster monomer diffusion processes in the LLDPE increases with increasing chamber temperature, enhanced probability of grafting reaction of the monomer, results in higher GD. Owing to invariant initial monomer concentration, GE also increases with increasing GD.

**Effect of Reaction Time.** Type-S curve of growth of GD can be observed with extension of reaction time [Figure 3(d)]. During the initial stage of reaction, due to insufficient monomer diffusion, the collision probability of monomer molecules and macroradicals was restricted, resulting in slow growth of GD. After sufficient monomer diffusion of monomer, with extension of reaction time, the macromolecular peroxide was decomposing and the collision probability of monomer molecules and macroradicals was increasing meanwhile, and accordingly the growth of GD slowed gradually. During the later stage of reaction, monomer concentration became the main factor of controlling

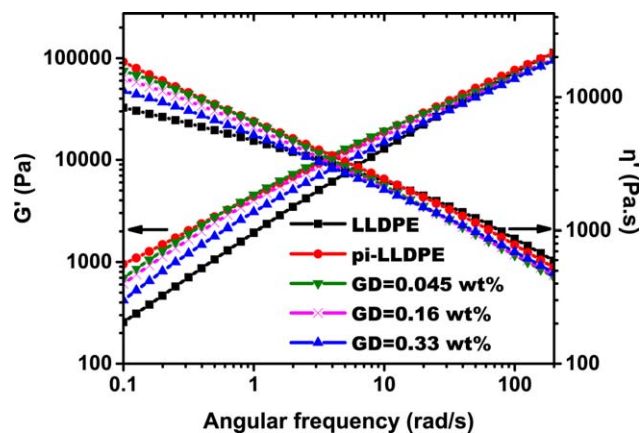


**Figure 4.** Dynamic viscosity ( $\eta'$ ) and storage modulus ( $G'$ ) as a function of frequency ( $\omega$ ) of the plain LLDPE, preirradiated LLDPE (pi-LLDPE), and LLDPE-g-MOANI with a series of grafting degree (GD) at 190°C. [Color figure can be viewed in the online issue, which is available at [wileyonlinelibrary.com](http://wileyonlinelibrary.com).]

owing to remarkable reduction of monomer concentration. The rate of grafting reaction was decreasing with further reducing of monomer concentration, as a result of slow growth of GD gradually.

The maximum GD is 0.4 wt % and the reason why GD of MOANI is so low was that chain transfer of hydrogen consists in allyl of MOANI consumed a lot of initial free radicals. But the allyl was chosen in order to inhibit homopolymerization of MOANI based on autoinhibition of allylic monomers ( $\text{CH}_2=\text{CH}-\text{CH}_2\text{Y}$ ).<sup>34</sup> The hypothetical reaction mechanism for MOANI grafting onto LLDPE in the melt is shown in Supporting Information Figure S4 and the similar mechanism was reported by Ciolino and coworkers.<sup>35</sup>

### Rheological Characterizations of LLDPE-g-MOANI

Samples of LLDPE-g-MOANI with a series of GD, preirradiated LLDPE and LLDPE were tested in SAOS-flow at low strain to determine the melt properties. Figure 4 shows the evolution of dynamic elastic modulus  $G'$  and dynamic viscosity  $\eta'$  ( $\eta' = G'/\omega$ , where  $G'$  denotes loss modulus<sup>36</sup>) with frequency for the plain LLDPE, preirradiated LLDPE, and selected LLDPE-g-MOANI samples. At the low-frequency range, the value  $G'$  and  $\eta'$  of the pre-irradiated LLDPE are higher than those corresponding to the plain LLDPE. This phenomenon is due to the weight-average molecular weight increment as a consequence of the predominance of chain-linking reactions. In the case of the LLDPE-g-MOANI, the value of  $G'$  and  $\eta'$  were reduced with respect to those values of the preirradiated LLDPE. The effect became even more substantial as the GD of MOANI in the LLDPE-g-MOANI increased. On the other hand, at the high-frequency range, elasticities of LLDPE, preirradiated LLDPE, and LLDPE-g-MOANI are similar but the melt viscosities of LLDPE-g-MOANI are lower than that of LLDPE and preirradiated LLDPE. The low melt viscosity of LLDPE-g-MOANI at high shear rates suggests that they have a broader MWD than LLDPE when the weight-average molecular weight of LLDPE-g-MOANI is higher than that of LLDPE. Moreover, this result

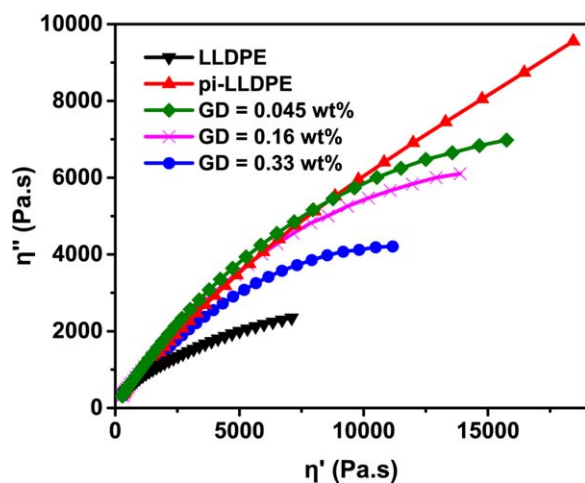


**Figure 5.** Cole–Cole plot of the plain LLDPE, preirradiation LLDPE (pi-LLDPE), and LLDPE-g-MOANI with a series of grafting degree (GD) at 190°C. [Color figure can be viewed in the online issue, which is available at [wileyonlinelibrary.com](http://wileyonlinelibrary.com).]

indicates that LLDPE-g-MOANI have well processability than LLDPE at high shear rates.

The rheological behavior of the graft LLDPEs can be further illustrated in the Cole–Cole plot consisting of out-of-phase viscosity  $\eta''$  ( $\eta'' = G'/\omega$ ) versus  $\eta'$  plot (Figure 5) clearly.<sup>37,38</sup> For the linear polymer molecule, the Cole–Cole plots were close to a semicircle, and the higher the molecular weight was, the bigger the radius was.<sup>37</sup> When there are long chain branches (LCB) on the backbone, the plot deviates from the semicircular shape, upturns at high viscosity, and the more evident upturning can qualitatively explain the more branching degrees of the polymer.<sup>38</sup>

As shown in Figure 5, the differences of these samples are very clear. For the plain LLDPE and LLDPE-g-MOANI with low GD, the Cole–Cole plots were close to a semicircle, and the lower the GD of MOANI was, the bigger the radius was. The radius of Cole–Cole plots of preirradiated LLDPE and LLDPE-g-MOANI with higher GD were bigger than that of the plain LLDPE as well as LLDPE-g-MOANI and showed more evident deviation from the semicircular shape at high viscosity. This phenomenon can be explained that the LCB, formed by low cross-linking of LLDPE backbones accompanying the graft of pre-irradiated LLDPE, is reduced or eliminated in the presence of MOANI, because the change of molecular weight caused by LCB is larger than that caused by graft of MOANI. These results suggested that the cross-linking of LLDPE can be inhibited effectively by graft of MOANI and the MOANI cannot polymerize to LCB. Although there is LCB, LLDPE did not cross-link since the gel was not found in the purification process.

#### Thermal Properties of LLDPE-g-MOANI

The isothermal crystallization behavior of polymers, as the development of crystallinity versus time, can be described by Avrami equation, which in its logarithmic form reads as

$$\log \{-\ln [1-x(t)]\} = n \cdot \log t + \log k \quad (4)$$

where  $x(t)$  is the relative crystallinity developed at time  $t$ ,  $k$  contains the rate constants of nucleation and crystal growth, and  $n$  reflects the type of nucleation and the habit of the growing nuclei. The kinetic parameters evaluated from the Avrami analysis are summarized in Table II, as usual, through the linear fitting of the first portion of the curve  $\log\{-\ln[1-x(t)]\}$  versus  $\log t$  in the case where a change in slope occurs. As an example, the Avrami plots of LLDPE-g-MOANI (GD = 0.4 wt %) obtained at different temperatures are shown in Supporting Information Figure S4. A similar trend was found for the other LLDPE-g-MOANI with different GD. Values of  $n$  in the range from 2.2 to 3.9 suggests that the crystallization (nucleating and growing) for all the above-mentioned materials should occur in the three dimensions.

As shown in Figure 6, values of crystallization half-time ( $t_{1/2}$ ) for the LLDPE was higher than anyone of LLDPE-g-MOANI determined at the same crystallization temperatures. It means that the crystallization rates of LLDPE-g-MOANI were higher than that of LLDPE. DSC cooling and melting traces of LLDPE-g-MOANI and the plain LLDPE for the sake of comparison are shown in Figure 7. The crystallization temperatures of LLDPE-g-MOANI and LLDPE/MOANI are located at higher temperature than the plain LLDPE [Figure 7(a)] and crystallinity of LLDPE-g-MOANI was increased with increasing GD of MOANI [Figure 7(b)]. These results indicate that the MOANI monomers grafted on LLDPE play the role of nucleating agents.<sup>39</sup>

The reason that there is not a decrease in  $t_{1/2}$  of LLDPE-g-MOANI with increasing GD is that LCBs as heterogeneous nucleation agents accelerate crystallization<sup>40</sup> and compete with MOANI.

#### Surface Morphologies of LLDPE-g-MOANI and LLDPE/MOANI Films

In order to demonstrate the blooming effect of MOANI in an LLDPE matrix and the beneficial effect of LLDPE-g-MOANI, LLDPE-g-MOANI (GD = 0.4 wt %) and LLDPE/MOANI with two content of MOANI (0.15 wt %, 0.25 wt %) were compared under the same conditions. The film surfaces were examined by SEM as shown in Figure 8. It can be clearly observed that toward LLDPE/MOANI, MOANI crystals have been formed on the film surface during the cooling stage and within 3 months of storage at room temperature. In contrast, no dye blooming effect could be noticed under the same conditions for the LLDPE-g-MOANI film. It turned out that the grafted MOANI could not migrate to the surface of the LLDPE-g-MOANI film.

#### Mechanical Properties of Unpurified LLDPE-g-MOANI Films as Function of UV Weathering Period

Mechanical properties of LLDPE, unpurified LLDPE-g-MOANI, and LLDPE/MOANI films as function of UV weathering period are shown in Figure 9, respectively. Before the test of UV weathering, no significant difference in the tensile strength and elongation at break was noted among the three films. After 48 h of exposure for the three films, LLDPE had lower tensile strength and elongation at break compared with the unpurified LLDPE-g-MOANI and LLDPE/MOANI films. In addition, a little

**Table II.** Isothermal Crystallization Kinetic Parameters of the Plain LLDPE and LLDPE-g-PPMM with a Series of Grafting Degree (GD) at Different Crystallization Temperature ( $T_c$ )

Sample	$T_c$ (°C)	N	K (min <sup>-n</sup> )	$t_{1/2}$ (min)
LLDPE	111	2.29556	0.042686	3.367734
	110	2.36429	0.05372	2.949684
	109	2.08553	0.137104	2.174986
	108	2.61626	0.180256	1.673312
	107	2.521	0.386216	1.261107
LLDPE-g-MOANI (0.07 wt %)	111	2.22331	0.099131	2.398231
	110	2.31748	0.159434	1.885406
	109	3.19311	0.272308	1.339909
	108	2.8458	0.475949	1.141223
	107	2.77133	0.651028	1.022878
LLDPE-g-MOANI (0.19 wt %)	111	2.3919	0.094463	2.300772
	110	2.64594	0.167121	1.711938
	109	3.02697	0.302099	1.315691
	108	2.97273	0.560415	1.074123
	107	2.96512	0.96241	0.89522
LLDPE-g-MOANI (0.40 wt %)	111	3.30376	0.064564	2.051251
	110	2.97309	0.155593	1.65286
	109	4.10934	0.31839	1.208423
	108	3.45923	0.529298	1.081082
	107	3.36674	1.079543	0.876695

change appeared on the tensile strength and elongation at break of the unpurified LLDPE-g-MOANI film of 0.25 wt % initial monomer concentration. These mean that MOANI acts as the role of ultraviolet absorber and inhibited the aging process of LLDPE. The photostabilizing efficiency gradually strengthens with the increasing concentration of MOANI and weakens with the photodegradation of MOANI. After 216 h, the tensile strength and elongation at break of all films decrease about 50%.

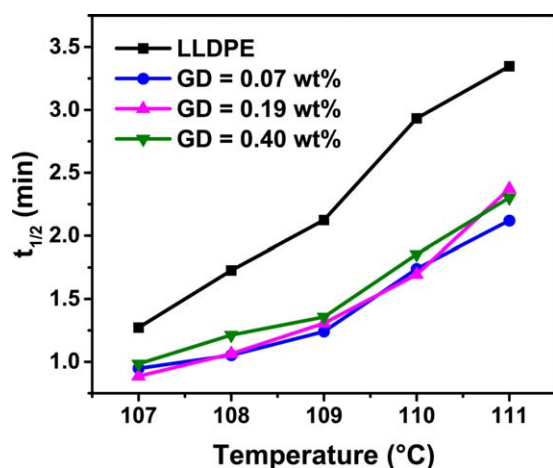


**Figure 6.** Half-time ( $t_{1/2}$ ) for crystallization of plain and graft LLDPE as a function of crystallization temperature ( $T_c$ ). [Color figure can be viewed in the online issue, which is available at [wileyonlinelibrary.com](http://wileyonlinelibrary.com).]

#### Fluorescent Properties of Unpurified LLDPE-g-MOANI Films as Function of UV Weathering Period

In this test, there are three environmental factors causing the fluorescent decay: UV irradiation, temperature, and condensed water on the surface of PE film. Except for the emission of fluorescence, MOANI can be photodegraded due to molecular matrix damaged by UV irradiation. The rise of temperature would accelerate the migration of free MOANI and promote the formation of its crystals on the PE surface, and these crystals would be rinsed by drips formed by condensed water on the film surface with their rolling down. Thereby, temperature and condensed water on the surface of PE film can cause the fluorescent decay.

Figure 10 shows the plot of the fluorescence retention ratios vs test time<sup>41</sup> in the UV weathering process of the MOANI in films. The retention ratios were calculated by the following equation:<sup>41</sup>

$$R_r = \frac{F_t}{F_0} \quad (5)$$

where,  $R_r$  = retention ratio,  $F_0$  = initial maximum fluorescence intensity at 0 day,  $F_t$  = maximum fluorescence intensity after  $t$  day test.

For LLDPE/MOANI films, the fluorescence retention ratios decreased exponentially as a function of test time; whereas for unpurified LLDPE-g-MOANI films, similar variation trend appeared from 0 to 120 h and the fluorescent decay strayed from this trend at the range of exceeding 120 h [Figure 10(a)].



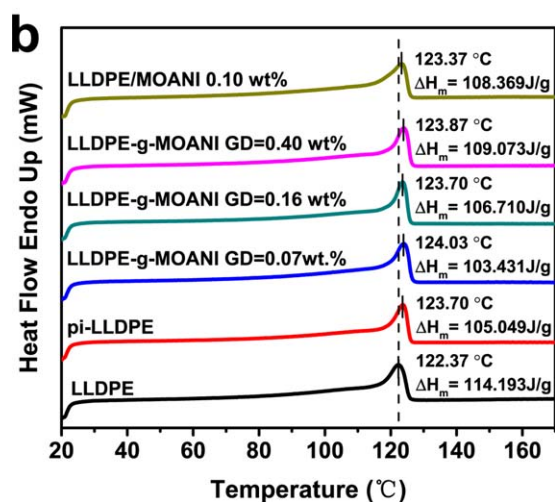
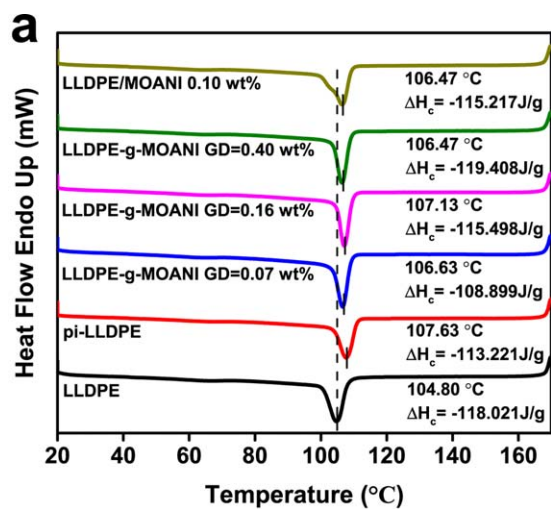


**Figure 7.** (a) DSC cooling and (b) melting traces of the plain LLDPE, pi-LLDPE, LLDPE/MOANI, and LLDPE-g-MOANI with a series of GD. [Color figure can be viewed in the online issue, which is available at [wileyonlinelibrary.com](http://wileyonlinelibrary.com).]

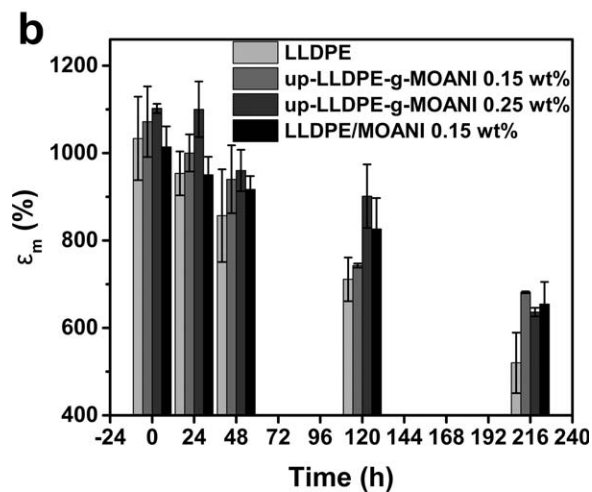
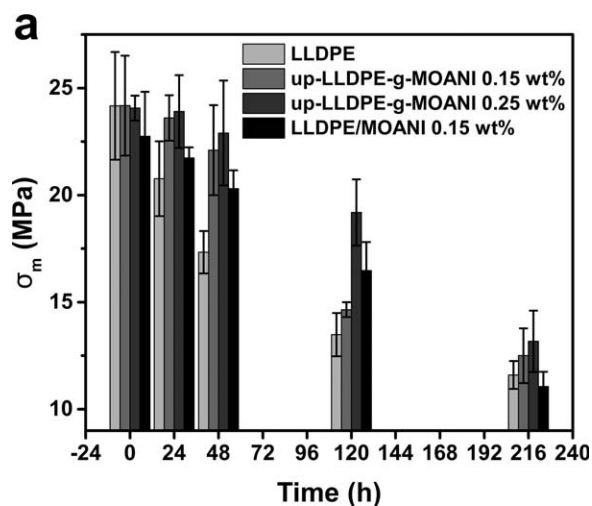


**Figure 9.** Changes in tensile strength ( $\sigma_m$ ) and elongation at break ( $\epsilon_m$ ) of LLDPE, LLDPE/MOANI and the unpurified LLDPE-g-MOANI (up-LLDPE-g-MOANI) films with two different initial monomer concentrations during UV weathering: (a) the tensile strength and (b) elongation at break of LLDPE.

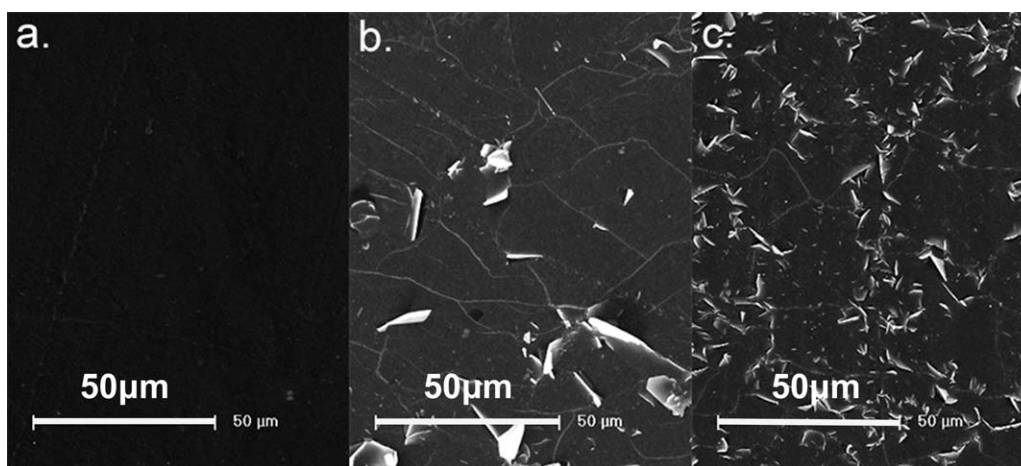


**Figure 8.** SEM micrographs of (a) LLDPE-g-MOANI (GD=0.4 wt %) and LLDPE/MOANI with the content of MOANI: (b) 0.15 wt %, (c) 0.25 wt %, after 3 months storage at room temperature.

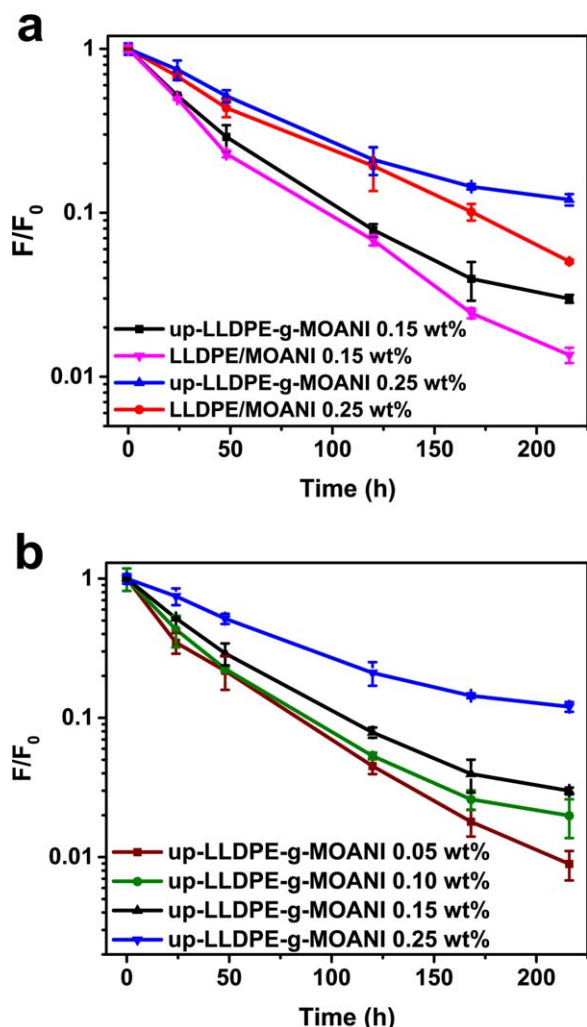


**Figure 10.** (a) Plot of the fluorescence retention ratios vs time in the UV weathering tests of the up-LLDPE-g-MOANI and LLDPE/MOANI films. (b) Plot of the fluorescence retention ratios vs time in the UV weathering tests of the up-LLDPE-g-MOANI films with different initial monomer concentration. [Color figure can be viewed in the online issue, which is available at [wileyonlinelibrary.com](http://wileyonlinelibrary.com).]

In addition, the deviation increasing with increasing content of MOANI as shown in Figure 10(b). The reason appearing deviation could be that the migration of the free MOANI was restrained by the grafted MOANI.

#### Migration of Free MOANI in Unpurified LLDPE-g-MOANI Films

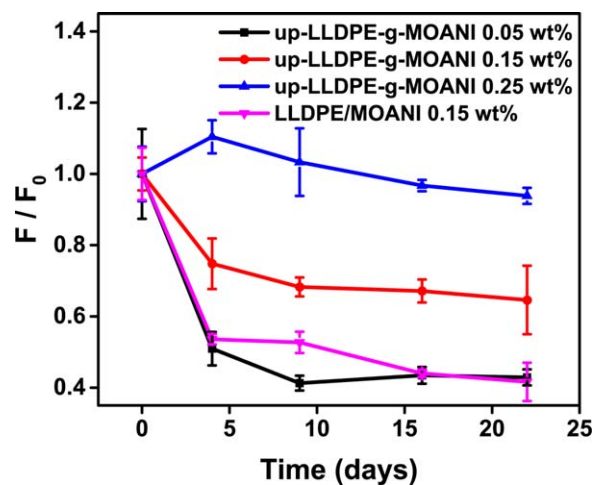
In the test of accelerated migration, just only two environmental factors—temperature and condensed water on the surface of PE film—can impact migration of MOANI in films, due to thermal motion of MOANI molecule and rinse of dripping formed by condensed water.

Figure 11 shows the plot of the fluorescence retention ratios vs time in the accelerated migration process of the MOANI in films. It was found that the fluorescent decayed rate of unpurified LLDPE-g-MOANI films was smaller than that of LLDPE/MOANI films in the same initial concentration of MOANI.

Furthermore, the lower the initial concentration of MOANI was, the faster the fluorescent decay of unpurified LLDPE-g-MOANI became. Above results suggested that the migration of the free MOANI in films was delayed by the grafted MOANI in films, due to existence of the intermolecular dipole–dipole interactions<sup>33</sup> between the free MOANI and the grafted MOANI (MOANI belonging to one of 1,8-naphthalimide derivatives is a donor– $\pi$ –acceptor [D– $\pi$ –A] bipolar molecule<sup>42</sup>). Moreover, the reason why the fluorescence retention ratio of 0.25 wt % unpurified LLDPE-g-MOANI at fourth and ninth day exceeded 1 is that the fluorescence concentration quenching occurred at 0 day.

#### CONCLUSIONS

MOANI has been synthesized using a one-pot method and successfully grafted onto molten preirradiated LLDPE obtained by  $\beta$ -ray irradiance in a mixer or single-screw extruder. The GD was determined by the UV/Vis spectra. The grafting degree of MOANI in LLDPE-g-MOANI increased with increasing MOANI monomer concentration, temperature, and reaction time. The initial monomer concentration and chamber temperature are the main processing parameters for controlling the grafting degree. The rheological behavior of LLDPE-g-MOANI suggests that the cross-linking of LLDPE can be inhibited effectively by graft of MOANI and the MOANI cannot polymerize to LCB. In addition, this result also shows that LLDPE-g-MOANI has well processability than LLDPE at high shear rates. The grafted MOANI monomer acts as a nucleation agent, which improves the crystallization rates of LLDPE molecular chains. Surface morphologies of LLDPE-g-MOANI and LLDPE/MOANI demonstrating the grafted MOANI are difficult to migrate to the surface of the LLDPE-g-MOANI film. Mechanical properties of unpurified LLDPE-g-MOANI films as function of UV weathering period mean that MOANI acts as the role of ultraviolet absorber and inhibited the aging process of LLDPE. The test results of accelerated migration and UV weathering indicate that migration processes of the free MOANI in unpurified



**Figure 11.** Plot of the fluorescence retention ratios vs time in the accelerated migration tests of the LLDPE/MOANI film and up-LLDPE-g-MOANI films with different initial monomer concentration. [Color figure can be viewed in the online issue, which is available at [wileyonlinelibrary.com](http://wileyonlinelibrary.com).]

LLDPE-g-MOANI films were delayed effectively by the grafted MOANI in these films. Real images of LLDPE-g-MOANI film and LLDPE/MOANI film are shown in Supporting Information Figure S6 under sunlight and UV 364 nm. It is expected that the modified LLDPE could be a promising candidate for long-term light converting films.

## ACKNOWLEDGMENTS

The authors would like to acknowledge the financial support of the National Natural Science Foundation of China (Project No 50873101) and the Support Project of National Science and Technology of China (Project No 2012BAD11B01-3).

## REFERENCES

1. Lamnatou, C.; Chemisana, D. *Renew. Sust. Energ. Rev.* **2013**, *27*, 175.
2. Hemming, S.; van Os, E. A.; Hemming, J.; Dieleman, J. A. *Eur. J. Hortic. Sci.* **2006**, *71*, 145.
3. White, A. L.; Jahnke, L. S. *Plant Cell Physiol.* **2002**, *43*, 877.
4. Novoplansky, A.; Sachs, T.; Cohen, D.; Bar, R.; Bodenheimer, J.; Reisfeld, R. *Sol. Energ. Mat.* **1990**, *21*, 17.
5. Pearson, S.; Wheldon, A. E.; Hadley, P. *J. Agr. Eng. Res.* **1995**, *62*, 61.
6. Espí, E.; Salmerón, A.; Fontecha, A.; García, Y.; Real, A. I. *J. Plast. Film Sheet* **2006**, *22*, 85.
7. Kosobryukhov, A. A.; Kreslavski, V. D.; Khramov, R. N.; Bratkova, L. R.; Shchelokov, R. N. *Biotronics* **2000**, *29*, 23.
8. Meng, J. W.; Meng, R. E.; Mang, Y. D.; Cao, B. C.; Li, W. *Spectrosc. Spect. Anal.* **2004**, *24*, 333.
9. Golodkova, L. N.; Lepaev, A. F.; Dmitriev, V. M.; Zhavoronko, N. M.; Ziskin, G. L.; Izmailov, G. I.; Ippolitov, E. G.; Karasev, V. E.; Troitskaya, L. S.; Troitsky, B. B.; Zhavoronkov, N. M.; Kirilenko, V. V.; Tsivadze, A. J.; Schelokov, R. N.; Tskhakaya, N. S.; Leplyanin, G. V.; Murinov, J. I.; Nikitin, J. E.; Tolstikov, G. A.; Rafikov, S. R.; Karaseva, E. T. (ASGE-Soviet Institute). U.K. Patent GB2158833-A, November 20, **1985**.
10. Heitzman, S. Colorants. In: *Encyclopedia of Polymer Science and Technology*, Volumes 1-4, Part 1, 3rd Edition; Mark, H. F., Ed.; Wiley: New York, **2002**; Vol. 2, pp 45.
11. Sun, L.; Fu, L.; Liu, F.; Peng, C.; Guo, J.; Zhang, H. *Chinese J. Lumin.* **2005**, *26*, 15.
12. Miao, L.; Ma, Y. L.; Xu, R. S.; Yan, W. *Environ. Earth Sci.* **2011**, *63*, 501.
13. Burkinshaw, S. M.; Froehling, P. E.; Mignanelli, M. *Dyes Pigments* **2002**, *53*, 229.
14. Hariri, K.; Ruch, T.; Riess, G. *E-Polymers* **2009**, *9*, 776.
15. Grabchev, I.; Moneva, I. *J. Appl. Polym. Sci.* **1999**, *74*, 151.
16. Mallakpour, S.; Rafiemanzelat, F.; Faghihi, K. *Dyes Pigments* **2007**, *74*, 713.
17. Konstantinova, T. N.; Miladinova, P. M. *J. Appl. Polym. Sci.* **2009**, *111*, 1991.
18. Breul, A. M.; Hager, M. D.; Schubert, U. S. *Chem. Soc. Rev.* **2013**, *42*, 5366.
19. Yao, Z.; Yin, J.; Song, Y.; Jiang, G.; Song, Y. *Polym. Bull.* **2007**, *59*, 135.
20. Li, W.; Yao, Z.; Jiang, G.; Zheng, X.; Li, L.; Yin, J. *J. Macromol. Sci. B.* **2010**, *49*, 75.
21. Xin, Z.; Yan, S.; Du, B.; Du, S.; Liu, C.; Stagnaro, P. *Des. Monomers. Polym.* **2014**, *17*, 746.
22. Zollinger, H. *Color Chemistry: Syntheses, Properties; Applications of Organic Dyes and Pigments*; Wiley: New York, **2003**.
23. Grabchev, I.; Konstantinova, T. *Dyes Pigments* **1997**, *33*, 197.
24. Triboni, E. R.; Berlinck, R. G. S.; Politi, M. J.; Berci Filho, P. *J. Chem. Res.* **2004**, *2004*, 508.
25. Shi, Q.; Zhu, L.; Cai, C.; Yin, J.; Costa, G. *J. Appl. Polym. Sci.* **2006**, *101*, 4301.
26. Shi, Q.; Zhu, L. C.; Cai, C. L.; Yin, J. H.; Costa, G. *Polymer* **2006**, *47*, 1979.
27. Harper, C. A. *Modern Plastics Handbook*; McGraw-Hill: New York, **2000**.
28. DIN EN ISO 527-3:1995/Cor 2:2001, *Plastics – Determination of tensile properties – Part 3: Test conditions for films sheets*. ISO, 2002.
29. Hallén, Å.; Wesslén, B. *J. Appl. Polym. Sci.* **1996**, *60*, 2495.
30. Yang, J.; Yao, Z.; Shi, D.; Huang, H.; Wang, Y.; Yin, J. *J. Appl. Polym. Sci.* **2001**, *79*, 535.
31. Verbeek, C. J. R.; Hanipah, S. H. *J. Appl. Polym. Sci.* **2010**, *116*, 3118.
32. Marini, A.; Muñoz-Losa, A.; Biancardi, A.; Mennucci, B. *J. Phys. Chem. B* **2010**, *114*, 17128.
33. Anslyn, E. V.; Dougherty, D. A. *Modern Physical Organic Chemistry*; University Science: New York, **2006**, *168*, 895, 899, 901, 954.
34. Odian, G. In *Principles of Polymerization*; Wiley: Hoboken, NJ, **2004**; p 198-349.
35. Ciolino, A.; Vallés, E. M.; Failla, M. D. *J. Appl. Polym. Sci.* **2004**, *92*, 2303.
36. Dordinejad, A. K.; Jafari, S. H. *Polym. Eng. Sci.* **2014**, *54*, 1081.
37. Tian, J.; Yu, W.; Zhou, C. *Polymer* **2006**, *47*, 7962.
38. Li-juan, L. O. U.; Jian-ye, L. I. U.; Wei, Y. U.; Chi-xing, Z. *Polym. Bull.* **2009**, *15*.
39. Pritchard, G. *Plastics Additives: An A-Z Reference*; Netherlands: Springer: London, UK, **1998**; p 466.
40. Tian, J.; Yu, W.; Zhou, C. *J. Appl. Polym. Sci.* **2007**, *104*, 3592.
41. Grabchev, I.; Staneva, D.; Betcheva, R. *Polym. Degrad. Stab.* **2006**, *91*, 2257.
42. Jin, R. F.; Tang, S. S.; Sun, W. D. *Tetrahedron* **2014**, *70*, 47.